MECHANICAL ANALYSIS OF REINFORCED PLATE STRUCTURES

Gábor M. Vörös
Department of Applied Mechanics, Budapest University of Technology and Economics
H-1512. Budapest, Hungary, *E-mail: voros@mm.bme.hu*

Abstract: The paper presents the development of a new plate/shell stiffener element and the subsequent application in determine buckling loads and modes of different stiffened panels. The formulation of the stiffener is based on a general beam theory, which includes the constraint torsional warping effect and the second order terms of finite rotations. As part of the validation of the method, complete shell finite element analyses were made for stiffened plates.

Keywords: *Stiffener, Free vibration, Buckling load, Constraint torsion.*

1. INTRODUCTION

Many mechanical engineering structures consist of stiffened thin plate and shell parts to improve the strength/weight ratio. The buckling and vibration characteristics of stiffened plates and shells subjected to initial or dead loads are of considerable importance to mechanical and structural engineers.

Among the known solution techniques, the finite element method is certainly the most favourable. It is a common feature of the finite element based methods that in order to attain displacement continuity, a rigid fictitious link is applied to connect one node in the plate element to the beam node shearing the same section. The rigid link approach neglects the out-of-plane warping displacements of the beam section and this is why the usual formulation overestimates the stiffener torsional rigidity. It is known, that during torsion the beam section does not remain plain. If this torsional warping is restricted by constraints, then the rate of torsion will also change along the beam axis. The theory of constraint torsion was developed by Vlasov [1]. Investigations of stand-alone beam structures proved that an approximate or more accurate modelling of the torsional stiffness can considerably modify the results.

As the objective of this paper is to study the effect of constraint torsion the shear deformation of the stiffener is neglected and the formulation is based on the well-known *Bernoulli – Vlasov* theory. For the finite element analysis, the stiffener element has two nodes with seven degrees of freedom per node. In order to maintain displacement compatibility between the beam and the stiffened element, a special transformation is used, which includes the coupling of torsional and bending rotations and the eccentricity of internal forces between the stiffener and the plate/shell elements.

2. BEAM ELEMENT

In this work, the basic assumptions are as follows: the beam member is straight and prismatic, the cross-section is not deformed in its own plane but is subjected to torsional warping, rotations are large but strains are small, the material is homogeneous, isotropic and linearly elastic. Let us have a straight, prismatic beam member with an arbitrary cross-section as it is shown in Fig. 1. The co-ordinate axes y and z are parallel to the principal axes, marked as r and s. The positions of the centroid **C** and shear centre **S** in the plane of each section are given by the relative co-ordinates y_{NC}, z_{NC} and y_{CS}, z_{CS}. The external loads are applied along points **P** located y_{SP} and z_{SP} from the shear centre.

The virtual work principle for the beam structure subjected to initial stresses is expressed as

$$\delta\Pi = \delta\left(\Pi_L + \Pi_G + \Pi_{Ge} - W\right) = 0 \ , \tag{1}$$

where Π_L , Π_G, Π_{Ge} are the linear elastic strain energy, the energy change due to initial stress resultants and the potential energy due to eccentric initial nodal loads, respectively, and W is the work of load increments on incremental displacements. The first two terms of total potential (1) can be rewritten as:

$$\Pi_L = \frac{1}{2}\int_0^L \left[EAu'^2 + EI_r w''^2 + EI_s v''^2 + EI_\omega \alpha''^2 + GJ\alpha'^2 \right] d\,x \ , \tag{2}$$

$$\begin{aligned}\Pi_G = \frac{1}{2}\int_0^L \Big[& N\left(v'^2 + w'^2\right) + M_W\alpha'^2 + M_1\left(v''w' - v'w''\right) + M_2\left(v''\alpha - v'\alpha'\right) + M_3\left(w''\alpha - w'\alpha'\right) \\ & + \left(V_r w' - V_s v'\right)\alpha - 2\left(V_r v' + V_s w'\right)\left(\bar{u}' - v''y_{CS} - w''z_{CS}\right)\Big] dx \ .\end{aligned} \tag{3}$$

Displacement parameters are u, v, and w the translations in the x, y, and z directions of point **S** and α denote rotations (twist) about the shear centre axis parallel to x. In Eq. (2) E and G are the Young's and shear moduli, respectively. The initial stress resultants in Eq. (3) are: N the axial force, V_r and V_s the shear forces acting at the shear centre, M_1, and M_2, M_3 are the twisting and bending moments with respect to shear centre **S**, respectively, and M_W is known as the Wagner effect:

$$M_W = \int_A \left(\left(r - y_{CS}\right)^2 + \left(s - z_{CS}\right)^2 \right) \sigma_x \, dA = N\, i_p^2 + M_r\beta_r - M_s\beta_s \ . \tag{4}$$

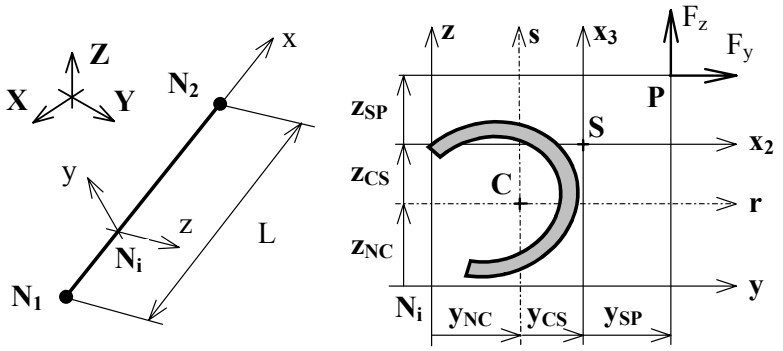

Fig.1. Beam element local systems and eccentricities

Also, sectional properties are defined as

$$I_r = \int_A s^2 \ dA \ , \quad I_s = \int_A r^2 \ dA \ , \quad I_\omega = \int_A \varphi^2 \ dA \ , \quad J = I_r + I_s - \int_A \left(s\frac{\partial\varphi}{\partial r} - r\frac{\partial\varphi}{\partial s} \right) dA \ ,$$

$$i_p^2 = \frac{I_s + I_r}{A} + {y_{CS}}^2 + {z_{CS}}^2 \ , \quad \beta_r = \frac{1}{I_r}\int_A s(r^2 + s^2) \ dA - 2z_{CS} \ , \quad \beta_s = \frac{1}{I_s}\int_A r(r^2 + s^2) \ dA - 2y_{CS} \ . \tag{5}$$

In these equations the warping function φ and the **S** shear centre location are the same as in the case of free torsion. For thin-walled sections $\varphi = -\omega$, the sector area co-ordinate.

The third term of Eq. (1) is the incremental work of initial external loads. Considering conservative initial forces F_x, F_y and F_z acting at point **P** (y_{SP}, z_{SP}) as signed on Fig. 1 of the i-th nodal section, the incremental work of these actions is

$$\Pi_{Ge} = -\frac{1}{2}\left[F_x\left(y_{SP}\beta + z_{SP}\gamma\right)\alpha + F_y\left(z_{SP}\beta\gamma - y_{SP}\left(\gamma^2 + \alpha^2\right)\right) + F_z\left(y_{SP}\beta\gamma - z_{SP}\left(\beta^2 + \alpha^2\right)\right)\right]_i \ . \tag{6}$$

The more detailed derivation of Π_L and Π_G, Π_{Ge} may be referred to Refs. [2] - [3].

2.1. Finite element model

The vector of seven local displacement and the element displacement parameters are defined as

$$\mathbf{\Delta}_i = \left[u, v, w, \alpha, \beta, \gamma, \vartheta\right]_i^T \quad , \quad \mathbf{U}_E = \left[\mathbf{\Delta}_1^T \quad \mathbf{\Delta}_2^T\right] .$$

A linear interpolation is adopted for the axial displacement and a cubic Hermitian function for the lateral deflections and the twist. Substituting the shape functions into Eqs. (2) and (3), and integrating along the element length *L*, elementary matrices can be defined as:

$$\delta\Pi_L = \delta\mathbf{U}_E^T\mathbf{k}_L\mathbf{U}_E \ , \quad \delta\Pi_G = \delta\mathbf{U}_E^T\mathbf{k}_G\mathbf{U}_E \ . \tag{7}$$

The explicit – exactly integrated – (14x14) element $\mathbf{k}_L$ linear stiffness and $\mathbf{k}_G$ geometric stiffness matrices can be found in Ref. [3].

3. STIFFENER TRANSFORMATION

Majority of publications using the finite element analysis of stiffened panels, where the stiffeners are modelled using beam elements, the beam nodes are forced to undergo the displacements and rotations prescribed by the corresponding plate/shell nodes. In this case the constraint condition is introduced by considering a rigid fictious link between the beam section and the plate/shell node **N** on the common normal. In such a model the displacements and rotations of a nodal point **N**, with the co-ordinates r = $-y_{NC}$ and s = $-z_{NC}$ (see Fig. 1) in the plane of the cross-section, will be as follows:

$$\begin{gathered} u_x = \bar{u} - \beta y_{NC} + \gamma z_{NC}, \quad u_y = v + \alpha\left(z_{NC} + z_{CS}\right) , \quad u_z = w - \alpha\left(y_{NC} + y_{CS}\right) , \\ \Theta_x = \alpha \ , \quad \Theta_y = \beta \ , \quad \Theta_z = \gamma \ , \end{gathered} \tag{8}$$

where u_x, u_y, u_z, Θ_x, Θ_y, Θ_z are the nodal local displacements and rotations. This transformation takes the eccentricity into account but obviously neglects the effect of torsional warping.

3.1 Continuity of rotations

If a beam is connected to another component not only in its cross-section but along a narrow stripe on its surface, the transformation (8) is not sufficient to assure the required displacement continuity. During torsion, while the cross-section turns around point **S** by an angle α, the originally straight connecting line crossing points **N** assumes a spiral shape. The rotation arising there is proportional to the distance between points **S** and **N**. Using the notations of Fig. 2, the vector of spiral rotation can be described as

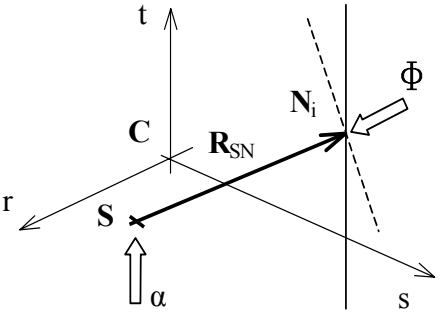

Fig. 2. Joint line rotation

$$\mathbf{\Phi} = -\frac{d\,\alpha}{dx}\ \mathbf{R}_{SN} = \vartheta\left(\mathbf{R}_{NC} + \mathbf{R}_{CS}\right) = \vartheta\begin{bmatrix} 0 \\ y_{NC} + y_{CS} \\ z_{NC} + z_{CS} \end{bmatrix}. \tag{9}$$

Supplementing bending rotations in Eq. (8) by these spiral rotation components:

$$\begin{gathered} u_x = \bar{u} - \beta y_{NC} + \gamma z_{NC}, \quad u_y = v + \alpha\left(z_{NC} + z_{CS}\right) , \quad u_z = w - \alpha\left(y_{NC} + y_{CS}\right) , \\ \Theta_x = \alpha \ , \quad \Theta_y = \beta + (y_{NC} + y_{CS})\vartheta \ , \quad \Theta_z = \gamma + (z_{NC} + z_{CS})\vartheta \ , \end{gathered} \tag{10}$$

which yields the modified transformation between the displacement parameters.

3.2. Eccentricity of internal forces

The calculation of $\mathbf{k}_{Ge}$ load stiffness matrix of the stiffener element requires some remarks. Initial internal forces or contact forces between the stiffener and the plating along the contact line can be calculated from the equilibrium condition of initial state. Hereinafter the contact point should be the node **N** and using the notation as indicated on in Fig. 1, the load eccentricities, if **N** = **P** are:

$$y_{SP} = y_{SN} = -\left(y_{NC} + y_{CS}\right), \quad z_{SP} = z_{SN} = -\left(z_{NC} + z_{CS}\right).$$

There is a simple way to calculate the stiffener load stiffness, if the cubic elements are used to define the initial stress state. It follows from the cubic shape functions that the N normal and V_r, V_s shear forces are constant along a straight beam element, but different from element to element. This internal force distribution can be produced by external forces acting at the two end nodes of an element:

$$F_{x1} = -N, \; F_{y1} = -V_r, \; F_{z1} = -V_s, \quad F_{x2} = +N, \; F_{y2} = +V_r, \; F_{z2} = +V_s. \tag{11}$$

With these end loads and eccentricities in Eq. (6), the additive stiffness due to off axis contact loads acting along the joint line is expressed as

$$\begin{aligned}\Pi_{Ge} = -\frac{1}{2}\Big[&\left(\alpha_1^2 - \alpha_2^2\right)\left(V_r y_{SN} + V_s z_{SN}\right) + \left(\beta_1^2 - \beta_2^2\right) V_s z_{SN} + \left(\gamma_1^2 - \gamma_2^2\right) V_r y_{SN} \\ &- \left(\alpha_1\beta_1 - \alpha_2\beta_2\right) N y_{SN} - \left(\alpha_1\gamma_1 - \alpha_2\gamma_2\right) N z_{SN} - \left(\beta_1\gamma_1 - \beta_2\gamma_2\right)\left(V_r z_{SN} + V_s y_{SN}\right)\Big].\end{aligned} \tag{12}$$

4. NUMERICAL ANALYSIS AND DISCUSSIONS

With the assembled system matrices the general equation for buckling problems is

$$\left[\mathbf{K}_L + \lambda\left(\mathbf{K}_G + \mathbf{K}_{Ge}\right)\right]\mathbf{U} = \mathbf{0},$$

where λ is the critical load parameter. The goal of the following numerical study is to compare the adequacy of two stiffener coupling transformations detailed in *Section 3*. First is the usual "rigid lever arm" coupling according to Eq. (8), and the other is the proposed stiffener coupling transformation including the internal force eccentricity in accordance to Eqs. (10) and (12). In the following these will be called of *BM* (beam) and *ST* (stiffener) coupling, respectively. In order to verify the *BM* and *ST* results of present study a COSMOS/M *shell* model was employed. In that model the plate and the thin walled beam was composed of the same four node *shell4t* thick shell element.

A rectangular stiffened panel on Fig. 3 consist of a flat plate with equally spaced thin walled T-stiffeners. Because of the symmetry in the structure, only a portion of the plate of width *b* with a T-stiffener, was modelled. In the finite element models the rotation about the longitudinal X axis and the lateral displacement were suppressed along the longitudinal edges to simulate the panel continuity and the X = 0 and X = *L* ends of the panel are fixed. The material properties are: E = 2.0 10^5 MPa, ν = 0.3. In order to model the wider range of behaviour of the panel, the plate dimensions and the beam shape unchanged, the area of stiffener was scaled in proportion to the web thickness. The cross sectional properties for the T-beam and the non-dimensional plate to beam area ratio parameter as the function of t_w are:

$$t_f = t_w, \quad b_f = 10 t_f, \quad b_w = 2 b_f, \quad A = 30 t_w^2, \quad I_r = 1402.5 t_w^4, \quad I_s = 85 t_w^4,$$

$$J = 10 t_w^4, \quad I_\omega = 0, \quad \beta_r = 16 t_w, \quad z_{NC} = -\left(13.5 t_w + 2\right), \quad z_{CS} = -7 t_w,$$

$$\delta = \frac{A_s}{A_p} = \frac{b_f t_f + b_w t_w}{bt} = \frac{t_w^2}{80}.$$

To investigate the effect of *BM* and *ST* coupling methods on the buckling loads and modes, the elastic buckling of the panel subjected to longitudinal compression is studied in this section. This kind of uniaxial compression can be produced by an U_{x0} axial displacement of the X = *L* end of the panel. Here, U_{x0} = 1 mm initial compression corresponds to

$$\sigma_{x0} = -U_{x0}\frac{E}{L} = -111{,}1 \text{ MPa}$$

initial normal stress.

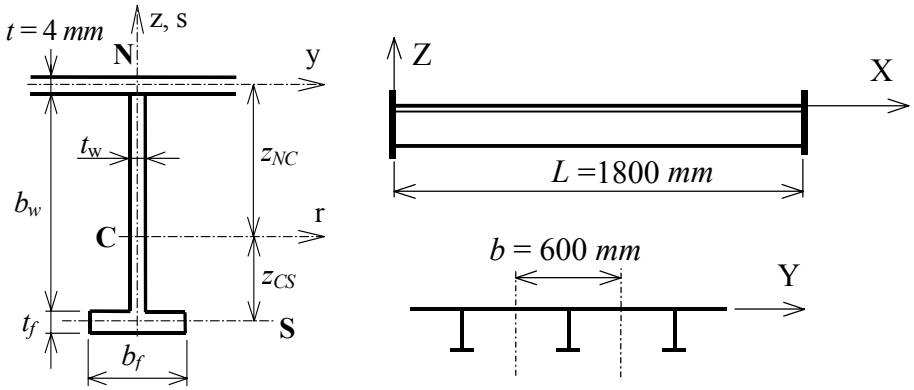

Fig. 3. Panel dimensions

The buckling mode shapes of the stiffened panel for different stiffener sections are shown in Fig. 4. The Fig. 5 shows the change of buckling modes and λ critical load parameter in terms of δ size parameter. If the stiffener section is small the buckling mode is the global (sometimes called of *Euler* buckling) flexural mode and the result is independent of the coupling (*BM* or *ST*) method. For higher stiffener sections torsional buckling mode, called of tripping will occur prior to flexural buckling. In contrast with flexural mode, there is a significant difference in the buckling loads of *BM-t1* and *ST-t1* coupling method, and the *ST* coupling results in a less rigid model with smaller critical loads. It is observed from the Table 1 that in case of δ = 0,2 the rate of decrease is around 30%. As the stiffener tripping is a coupled lateral torsional-bending motion, the accurate modelling of torsional properties are of great importance. A detailed analysis of the different buckling modes of stiffened panels, including the parametric analysis of tripping, can be found in recent papers of Yuren et al. [4] and Sheikh at. all. [5].

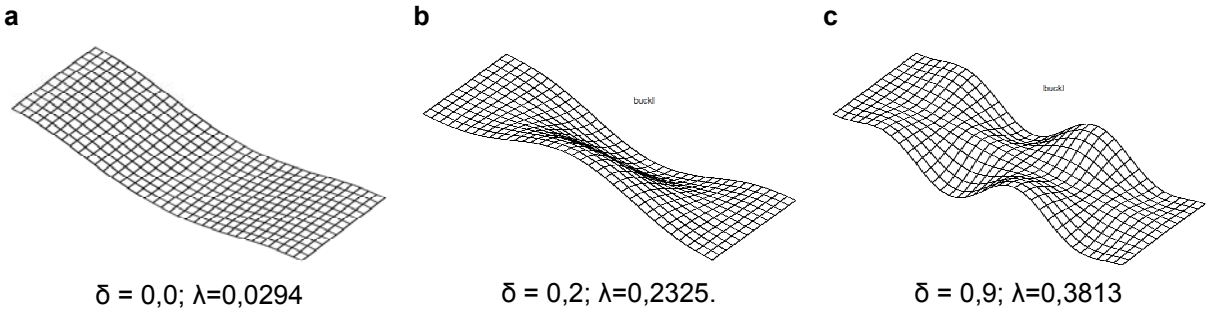

δ = 0,0; λ=0,0294 δ = 0,2; λ=0,2325. δ = 0,9; λ=0,3813

Fig. 4. Global (a), tripping (b) and plate buckling (c) modes.

With increasing stiffener size and rigidity the difference between *BM* and *ST* results vanish. The uniform asymptotic critical load in Fig. 5 indicates the buckling of plate between the stiffeners, as it is shown in Fig. 4. On Fig. 5 quite satisfactory agreement can be seen for the critical load parameter between the *ST* and COSMOS/M *shell* results marked with black dots.

δ / t_w (mm)	*BM* Eg. (8)	*ST* Eqs. (10, 12)	*shell* COSMOS/M
0.00 / 0.0	0.0294	0.0294	0.0293
0.20 / 4.0	0.3344	0.2325	0.2274

Tab. 1. Buckling load parameter λ.

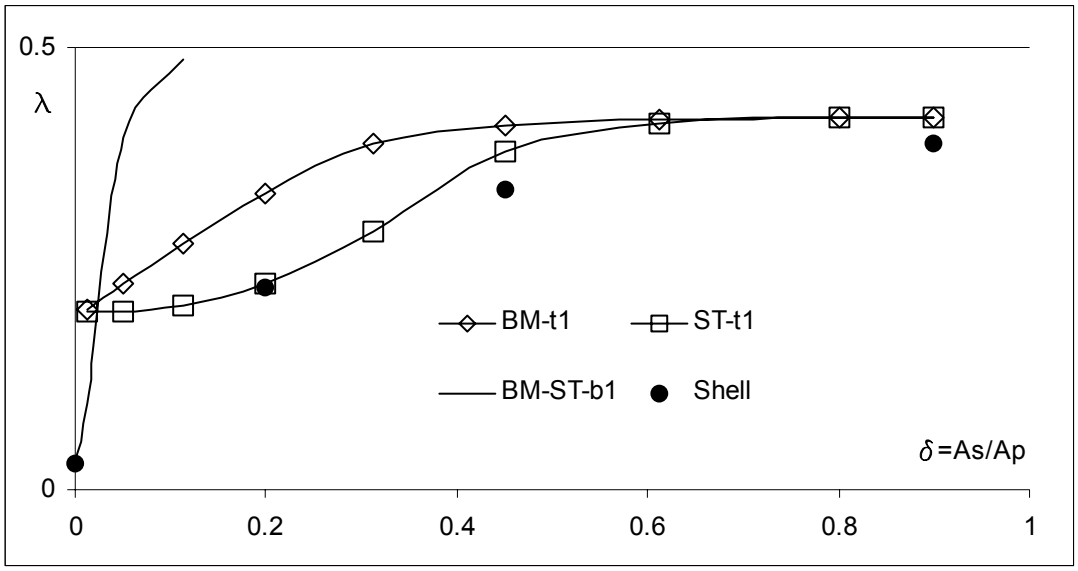

Fig. 5. Change of buckling modes and load parameter

5. CONCLUSIONS

In this study a detailed numerical evaluation has been performed to prove the efficiency of the proposed stiffener – plate/shell coupling method. It was shown that in all torsion related cases the proposed *ST* method leads to a less rigid model. The results show good agreement with complete shell solutions. This fact indicates that the application range can be extended. Though further work can be undertaken to perform dynamic and buckling analysis of really curved panels with stiffeners, the newly developed coupling method can be useful for future researches.

REFERENCES

[1] Vlasov VZ. Thin-walled elastic beams. National Science Foundation, Washington,1961.
[2] Kim MY, Chang SP, Park HG. Spatial postbuckling analysis of nonsymmetric thin-walled frames. I: Theoretical considerations based on semitangential property. J Engineering Mechanics (ASCE) 2001;127(8):769-78.
[3] Vörös, GM. An improved formulation of space stiffeners. Computers and Structures 2007;85(7-8):350-59.
[4] Yuren H, Bozen C, Jiulong S. Tripping of thin-walled stiffeners in the axially compressed stiffened panel with lateral pressure. Thin-Walled Structures 2000;37.1-26.
[5] Seikh IA, Elwi AE, Grondin GY. Stiffened steel plates under uniaxial compression. J. Constructional Steel Research 2002;58.1061-80
[6] Vörös, G.M. Buckling and Vibration of Stiffened Plates. International Review of Mechanical Engineering (I.RE.M.E.) 2007;1(1): 49-60.